LIMNOLOGY and OCEANOGRAPHY

ASLO

Limnol. Oceanogr. 70, 2025, 54–67

doi: 10.1002/lno.12734

Edge effects impact blue carbon dynamics across coastal ecotones in a tropical seascape

Erik S. Yando [1,2,3*] **Jahson B. Alemu I** [2,4] **Kiah Eng Lim** [2,5] **Taylor M. Sloey** [1,5] **Michiel van Breugel** [2,5,6] **Natasha Bhatia** [7] **Daniel A. Friess** [8]

[1]Department of Biological Sciences, Old Dominion University, Norfolk, Virginia, USA
[2]Department of Geography, National University of Singapore, Singapore
[3]Campus for Research Excellence and Technological Enterprise, Singapore
[4]School of Marine and Environmental Sciences, University of South Alabama, Mobile, Alabama, USA
[5]Yale-NUS College, Singapore
[6]ForestGEO, Smithsonian Tropical Research Institute, Panama City, Panama
[7]Asian School of the Environment, Nanyang Technological University, Singapore
[8]Department of Earth and Environmental Sciences, Tulane University, New Orleans, Louisiana, USA

Abstract

Coastal wetlands are important for their ability to regulate global climate through the sequestration and long-term storage of carbon. Accurate quantification of ecosystem-specific carbon dynamics (including sequestration, storage, and fluxes) is needed to develop accurate carbon budgets that inform climate change mitigation. Most work to quantify carbon dynamics either use subsampling in core habitats or benefit transfers to upscale values. While these approaches are valuable, our understanding of carbon dynamics across ecosystem transitions and overall heterogeneity remains a critical gap in coastal ecosystems as boundaries are not always clear. In this study, we established transects across both mangrove and seagrass ecotones into adjacent tidal flats in Singapore to quantifying vegetation cover, soil carbon storage, and CO_2 fluxes. Vegetation cover in all transitions and soil carbon storage in most transitions followed a decreasing sigmoidal pattern from vegetated to unvegetated portions, but differed in rate and width. CO_2 fluxes followed a peak distribution in mangrove–tidal flat transitions with maximum values occurring within the mangroves and were correlated with pneumatophore density, while seagrasses saw a linear increase in CO_2 fluxes from the seagrass to tidal flat. Seascape analysis of soil carbon showed site-specific impacts that resulted in differences in carbon stocks (0%–8%) as well as the width of these transitions. This study highlights the importance of understanding ecotones to better account for edge effects, which can lead to the over or under estimation of carbon, and provides a needed step in increasing the accuracy of blue carbon assessments in these critical ecosystems.

Coastal ecosystems are well known for the numerous ecosystem services they provide (Barbier et al. 2011). Recently, emphasis has been placed on their role in macroclimate regulation, with mangrove forests, salt marshes, and seagrass meadows drawing particular attention as these ecosystems can sequester and store a disproportionately large amount of carbon per area compared to many other ecosystems (McLeod et al. 2011; Taillardat et al. 2018). The carbon these systems sequester and store, coined as "blue carbon," and the quantification and comparison of blue carbon has been of increasing interest over the last decade (Lovelock and Duarte 2019; Macreadie et al. 2019). Researchers, practitioners, and governments alike depend on accurate estimates of blue carbon to evaluate carbon storage and sequestration, understand the ability of blue carbon systems to provide climate mitigation, and understand potential impacts of both restoration and disturbance. Estimates of blue carbon are often scaled up from local measurements to total ecosystem area, using a value transfer from regional data points, or less frequently by remote

*Correspondence: eyando@odu.edu

Additional Supporting Information may be found in the online version of this article.

Author Contribution Statement: ESY, NB, and DAF conceptualized the study. ESY, JBA, NB, DAF, and TMS designed the methods. ESY, JBA, LKE, and TMS collected the data. ESY, JBA, and MvB analyzed the data. ESY led the writing of the paper. All authors contributed critically to the drafts of this manuscript.

sensing approaches that are most suitable to model aboveground carbon stocks (vegetation biomass) (Young et al. 2021). Although these approaches provide a useful estimate of system-wide carbon budgets, they are limited in their ability to capture seascape heterogeneity (Sasmito et al. 2020), differences between above- and belowground contributions (Owers et al. 2022), and potential edge dynamics within and between the boundaries of blue carbon ecosystems.

Seascape position, edges/boundaries, and connectivity has long been investigated by foodweb and seascape scientists (Bostrom et al. 2011) and the potential impacts of outwelling (Odum 1968) has been a source of continued interest and debate for blue carbon ecosystems, their adjacent counterparts, and other systems further afield (e.g. Hyndes et al. 2014; Huxham et al. 2018; Krause et al. 2022). However, our understanding of the connectivity, overlap, and edge impacts in carbon pools across ecosystem transitions remains a critical gap in understanding blue carbon dynamics, particularly at the micro (1s–10s m)- and meso (10s–100s m)-spatial scale. Boundaries of ecosystems are inherently difficult to define (Holland et al. 1991; Strayer et al. 2003) as they may be discrete or gradual (Gosz 1993) and what is observed aboveground may or may not reflect belowground characteristics (Titlyanova et al. 1999). Although remote sensing techniques can provide information on some aboveground boundaries depending on the attributes being mapped and resolution; belowground properties and boundaries are far more difficult to capture, and may not correspond directly to vegetation cover or other metrics. Overlap may arise from plant-specific structures, such as roots of the dominant vegetation across the ecotone (Yando et al. 2018) or may also be a product of the ecosystem, such as nutrient subsidies and exchange (Wiens et al. 1985; Huxham et al. 2018; Bulmer et al. 2020). Moreover, belowground spatial patterns may reflect past ecosystems extents, geological processes, and disturbance events. Critical evaluation of the heterogeneity of carbon stocks and fluxes is needed particularly at habitat boundaries and at scales relevant to these edges.

Heterogeneity of blue carbon stocks and fluxes has been examined at a variety of scales between and within habitat patches and ecosystems. Previous work has focused on comparing patch variability within individual blue carbon ecosystems ranging from local studies to global comparisons and between ecogeomorphic settings (Ricart et al. 2017, 2020; Rovai et al. 2018). Additionally, prior studies have examined differences in carbon dynamics between multiple blue carbon ecosystems (e.g., mangrove vs. salt marsh vs. seagrass), made comparisons between blue carbon and blue carbon adjacent systems, or in a seascape approach (e.g., Simpson et al. 2019; Saavedra-Hortua et al. 2020). Far fewer studies, however, have examined within-patch heterogeneity in blue carbon ecosystems (e.g., mangrove—Kauffman et al. 2011; seagrass—Ricart et al. 2015; salt marsh—Arriola and Cable 2017). Both measurements of between- and within-patch differences provide important information of heterogeneity and help to improve estimates of carbon stocks and fluxes, while allowing for more appropriate scaling. However, these approaches typically focus solely on areas located within clearly distinct habitat patches of a particular ecosystem and largely ignore carbon dynamics within transitional ecotones between different vegetated patches (Yando et al. 2018; Engelbrecht et al. 2024) or into adjacent unvegetated patches (Sasmito et al. 2020). Ecotonal environments may be limited in their contribution to carbon accounting at the largest scales and in areas that have large continuous patches, but they are likely to have a more pronounced effect on carbon estimates in patchy environments or at smaller spatial scales where transitions and perimeter-area ratios are high. Further, it is important to consider ecotones in environments where change (rapid or slow) is occurring due to natural or anthropogenic factors, such as accretion, erosion, restoration, or sea level rise (Woodroffe et al. 2016).

We examined soil carbon stocks and carbon dioxide fluxes across two coastal ecotone types in Singapore: (1) the mangrove–tidal flat transition and (2) the seagrass-tidal flat transition. We specifically asked: (1) How do carbon stock and carbon dioxide flux measurements change across ecotonal transitions? (2) Do observed aboveground vegetation cover estimates correlate with belowground soil properties and processes across ecotonal transitions? (3) How can these measurements be scaled up in the coastal seascape from transects to patches to provide a more robust view of carbon stock estimates? Through exploring these questions in a concise geographic area that includes mangrove, seagrass, and tidal flat habitats, we aim to inform an understanding of local-scale carbon dynamics and heterogeneity in blue carbon seascapes, a necessary step for robust quantification of coastal carbon stocks and fluxes. Further, this work contributes to a broader understanding of ecotone dynamics in coastal seascapes.

Methods

Study site and experimental design

Our study was conducted in the Southeast Asian citystate of Singapore, with field sites focused on the Johor Strait which separates Singapore from Malaysia. This area is a tropical tidal estuary with mangroves occurring at median elevations from -0.1 m to $+1.5$ m relative to mean sea level (Leong et al. 2018), with supratidal elevations dominated by terrestrial vegetation or built infrastructure. Seagrasses are found in the low intertidal and subtidal portions of the tidal frame and often co-occur with patchy corals and tidal flats. Our study examined these coastal vegetated to unvegetated ecotones (Fig. 1) with a focus on understanding the patterns of carbon dynamics across transition zones (Fig. 1a). Coastal development in Singapore has led to the loss of more than 90% of mangrove forest (Lai et al. 2015), 45% of seagrass (Yaakub et al. 2014), and $\sim$ 75% of tidal flat habitats (Lai et al. 2015). Common disturbances in the past have included conversion

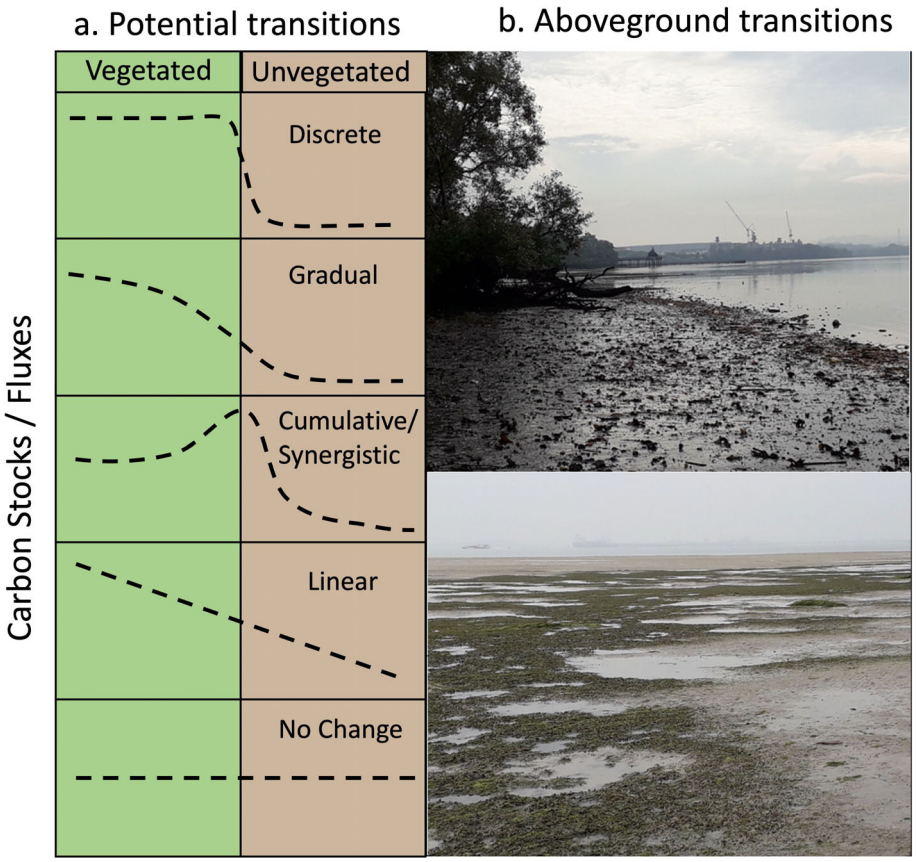

Fig. 1. (**a**) Potential ecotonal transitions (not exhaustive) of carbon stocks and fluxes between vegetated and adjacent unvegetated ecosystems. The shape of the curve may be metric-specific even within the same ecotone. (**b**) Aboveground ecotone for mangrove to tidal flat and seagrass to tidal flat. Photos: top—Sungei Buloh Wetland Reserve, Singapore; bottom—Chek Jawa, Pulau Ubin, Singapore.

to freshwater reservoirs, land reclamation, infrastructure, and aquaculture (Hilton and Manning 1995; Friess 2017). However, Singapore still maintains 931.1 ha of mangroves, 229.6 ha of seagrass (meadows and seagrass/algae mixes), and 636.3 ha of tidal flats (Tan et al. 2023). Species diversity of vegetation is relatively high in Singapore's coastal ecosystems, with more than 35 species of mangrove (Yang et al. 2011) and 15 or more species of seagrass present (Yaakub et al. 2014).

Singapore receives an average of 2113 mm of rainfall per year, maintains a tropical climate, and has two monsoon seasons each year (Meteorological Service of Singapore 2024). The Johor Strait has mixed semi-diurnal tides that reach 3–3.5 m during spring tides depending on location (Wyrtki 1961; Behera et al. 2013) with varying amounts of freshwater inputs due to damming and other impoundments restricting waterflow into and across these waterways. The Johor-Singapore Causeway is particularly important, which limits exchange to the western half of the Strait.

At three locations we established transects ($n = 3$) running from vegetated habitats (mangrove or seagrass) into the surrounding unvegetated habitats (tidal flat) (Chek Jawa on Pulau Ubin, Sungei Puaka on Pulau Ubin, and at the Sungei Buloh Wetland Preserve, Singapore) (Fig. 1b). Selected locations represented spatial variation in hydrogeomorphic settings and vegetation communities, with Chek Jawa representing a sandy coastal seagrass habitat, Sungei Puaka representing an open tidal channel mangrove to tidal flat habitat in northeast Singapore, and Sungei Buloh representing an estuarine mangrove to tidal flat habitat in Singapore's northwest coastline (Fig. 2a). Additionally, these three sites are representative of Singapore's larger contiguous coastal habitats and are less fragmented than other urbanized and/or fringing coastal areas. All transects ran perpendicular to the edge of each vegetated habitat. Plots of 1 m^2 (1 m × 1 m) size were placed systematically along each transect, with one plot located at the transitional aboveground boundary between habitats (0 m), and additional plots located 1, 2, 4, and 8 m extending from either side of the boundary into the adjacent vegetated (negative values; Fig. 2b) or unvegetated areas (positive values; Fig. 2b). An additional plot was also established at either end of the transect within the respective habitat where possible. These plots were established to serve as an endpoint located within a distinct habitat patch (i.e., not within the ecotone), and thus the location of these points differed in distance from the

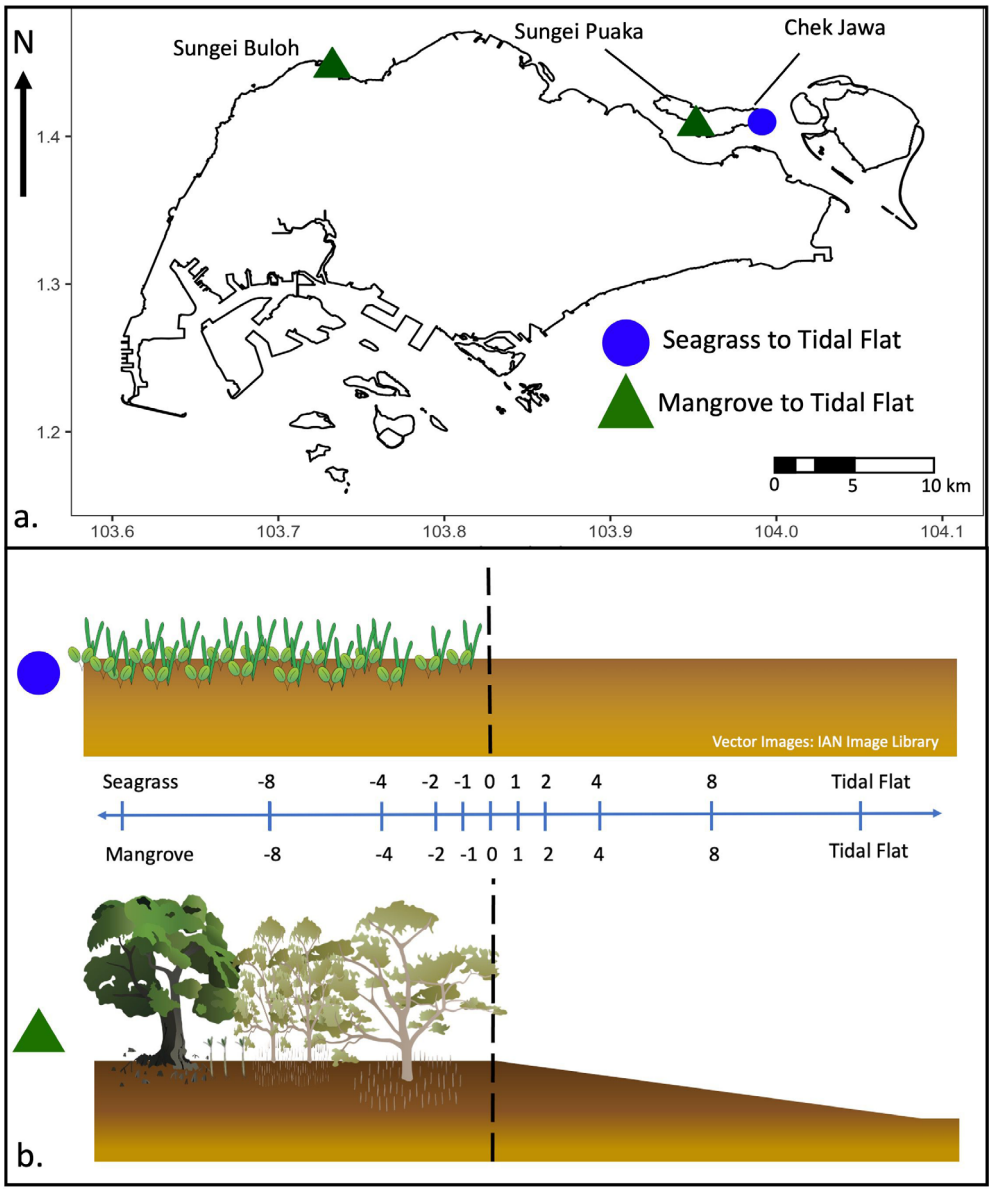

Fig. 2. (**a**) Map of Singapore with study locations listed: Sungei Buloh, Sungei Puaka, and Chek Jawa (three transects per location). Green triangle = mangrove to tidal flat transitions and blue circles = seagrass to tidal flat transitions. (**b**) Depiction of transects and plot locations from vegetated (seagrass and mangrove) to unvegetated (tidal flat) with aboveground transition listed at 0 m mark (dashed line). Three transects were established at each sampling location indicated on the map ($n = 3$). Plots were marked every few meters along the transect with negative numbers representing plots in vegetated habitat, and positive numbers representing plots in nonvegetated habitat.

transition point depending on the habitat patch size so as not to approach other nearby patches or ecotones (e.g., interior tidal channel, upland, intertidal corals) (Fig. 2b) (endpoint locations: Chek Jawa—seagrass: −20, −26, −38 m; Chek Jawa—tidal flat: not possible at any of the three transects; Sungei Buloh—Mangrove: −13, −19, -22 m; Sungei Buloh—tidal flat: 22, 25 m, not possible for one transect; Sungei Puaka—mangrove: −16, −20, −32 m; Sungei Puaka—tidal flat: 18, 22, 22 m).

Vegetation metrics

In transects with mangroves, aboveground metrics included average canopy cover measured using a convex spherical densiometer (Model No. 43887, Forestry Suppliers Inc.). To limit estimation errors across the transition, two measurements on either side of the transect were averaged to avoid landward and seaward cover influences. Pneumatophore density was measured in a 0.25-m^2 quadrat centered in each plot. In transects with seagrass, aboveground metrics included total

seagrass cover which was visually assessed in a 1-m^2 quadrat centered on each plot. Visual assessments were suitable for this site due to the limited number of species, the intertidal position of the seagrasses, the relatively small size of the quadrat, and were always conducted by same individuals to reduce variability.

Soil carbon storage and soil metrics

Soil carbon storage was determined at all points along the transect by collecting a 1-m long (5.08-cm diameter) soil core using a gouge auger. Cores were divided into four sections (0–15, 15–30, 30–50, and 50–100 cm) (sensu Kauffman and Donato 2012) in the field and a 5-cm long subsection was collected from the midpoint of each section. Soil samples were brought back to the lab, weighed (wet), and stored at 4°C prior to processing. All soil samples were dried at 60°C until constant mass was achieved, weighed (dry), and homogenized and ground using a ball mill. For each sample, the moisture (%) was calculated using wet mass and dry mass, and bulk density (g cm^{-3}) was calculated using the dry mass and the volume of each soil segment. Carbon analyses were completed using an elemental analyzer (vario TOC cube, Elementar Inc.) to provide total carbon of each sample. An additional sample from each segment was run through the elemental analyzer after being exposed to an acidified atmosphere for 24 h, irrigated with ultra-pure water, and dried at 60°C prior to analysis to remove all inorganic carbon (carbonate) and provide total organic carbon (TOC) values. Total inorganic carbon was calculated by the difference between total carbon and TOC. All samples were analyzed twice in the elemental analyzer and averaged. Carbon stock in kilograms per square meter was calculated to make suitable comparisons (similar to Howard et al. 2014) using corer area down to 1 m. All averaged data can be found in Supporting Information Table S1.

Atmospheric CO_2 flux at soil surface

Along the previously described transects we measured net carbon dioxide flux at all plots using a LI-COR 6800 (LI-COR) portable photosynthesis system with adjoining soil flux chamber (LI-COR 6800-09) (diameter: 20 cm) at low tide. All measurements were completed on a combination of either a 10-cm soil collar or the soil collar and a closed cell foam mat to ensure reduced sinking in the soft coastal sediments (*see* Supporting Information Fig. S1 for all dimensions and specifications of two mats used). Duplicate measurements were taken at each sampling time and location and subsequently averaged, values where obvious issues with the chamber seal or moisture were evident were removed prior to analysis. Measurements were taken in February and March 2020 and again in January and February 2021 to account for interannual variation in net flux. For seagrass and tidal flat systems, the net CO_2 flux represents the entire ecosystem (plant, if present, and soil), while for the mangrove systems it represents soil and pneumatophore, if present, flux.

Mapping of carbon stocks across the local seascape

To examine how scaling up and seascape arrangement influence an ecotone-specific assessment of carbon stocks compared with traditional interior habitat-based estimates, we chose to map our carbon stock data across each sampling location with the goal of highlighting the magnitude and location of differences. Using a coastal habitat extent map from 2015 to 2017 (Tan et al. 2023) we cropped relevant areas based on natural geographic boundaries (adjacent upland, shallow water, or other habitat boundaries) for our areas of interest. For all simple calculations we applied carbon stock values at kilograms per square meter to each habitat type using the average of all measurements at 8 m or more from the transition for each habitat type. For all calculations using our ecotone measurements, we calculated distance from the boundary across the local landscape and then calculated carbon stocks at a 1-m^2 resolution using the terra (Hijmans 2023), landscapeR (Masante 2016), and leaflet (Cheng et al. 2022) packages in R Studio (version 4.2.0) based on the TOC values from the TOC stock regressions calculated in this study (see Data analysis section; Yando et al. 2024). Additionally, the difference between the simple carbon estimate and the ecotone carbon estimate was calculated (simple carbon – ecotone carbon) and plotted to highlight areas of the largest differences present.

Data analysis

Independent variables included plot distance and pneumatophore density and dependent variables included mangrove cover, seagrass cover, carbon dioxide flux, and TOC stocks. All data were assessed for quality and control prior to analysis. Regression models were selected by R^2 in SigmaPlot using regression modules. When similar, the simplest and most ecologically suitable models were selected. For sigmoidal regressions, the inflection point (first derivative) and area of change (second derivatives) were calculated to identify the location and width of the transition [sigmoidal equation used $f = y0 + a/1 + \exp(-[x - x0]/b)$]. For additional information regarding this workflow and calculating inflection points and area of change *see* Timoney et al. 1993 and Hufkens et al. 2008. Mixed effect models were used on flux data to determine if year was a significant factor for its comparisons on transects in RStudio. Since year was not significant and year-to-year differences were not the focus of the analysis, regression models (linear and Lorentzian peak) were used instead. For Lorentzian peak models, peak maximums (y maximum), peak position (x value at y maximum), and peak width were calculated. Peak width was calculated using half width of half peak maximum to provide a standardized measurement of Lorentzian peak width (y maximum/2 = $x1$ and $x2$ → distance from $x1$ to $x2$ = full peak width of half peak maximum → full peak width of half peak maximum/2 = half peak width of half peak maximum) (example code present in Yando et al. 2024). Model confidence for all analyses was assessed using 95% confidence intervals, R^2 values, AICc values, and F-values where suitable

(Nakagawa et al. 2017). Analyses were conducted in RStudio (Team RStudio 2024) and SigmaPlot (Systat 2023).

Results

Vegetation metrics

Seagrass cover followed a sigmoidal decrease from across the aboveground transition from seagrass plots (60%) to tidal flat plots (0%) (Fig. 3a; Table 1). The inflection point was located at − 0.04 m on the transect with a narrow transition zone of ∼ 30 cm based on the model, but confidence intervals highlight a large amount of uncertainty due to variability at this transition (Fig. 3a; Table 1). Mangrove cover in both the Sungei Buloh and Sungei Puaka locations also decreased in a sigmoidal manner from inner mangrove sampling plots (∼ 100%) to the surrounding tidal flat (0%) (Fig. 3; Table 1). Both locations had similar inflection points at 0.84 m (Sungei Buloh) and 0.66 m (Sungei Puaka), but the area of transition was 50%–60% wider at Sungei Buloh compared to Sungei Puaka with less uncertainty compared to seagrass models (Fig. 3; Table 1). When compared to interior locations (< −8 m) both locations achieved comparable mangrove cover within 4 m of the aboveground transition.

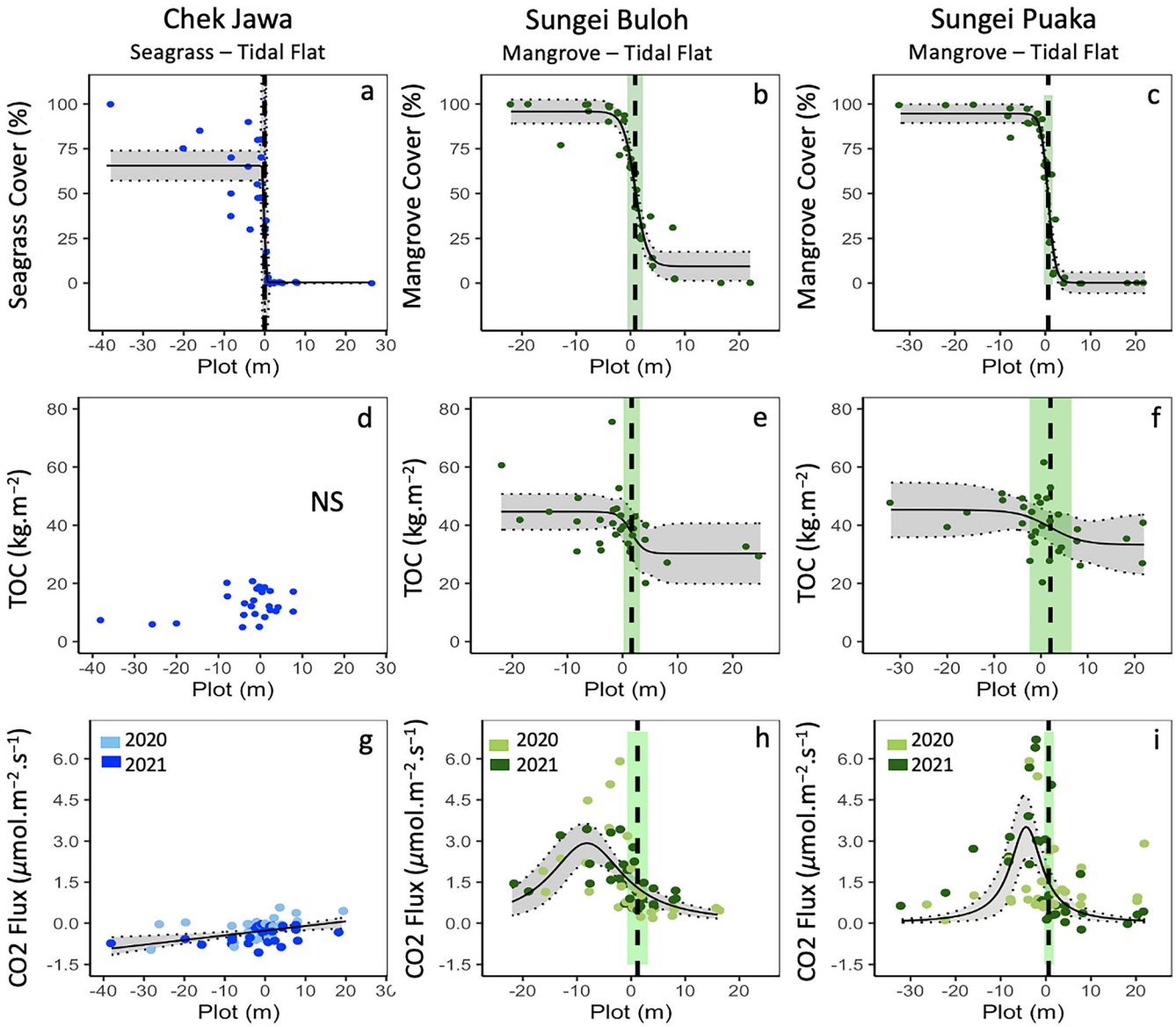

Fig. 3. Aboveground cover (%), total organic carbon (kg m^{-2}), and carbon dioxide flux (μmol m^{-2} s^{-1}) across the vegetated–unvegetated boundary at Chek Jawa—seagrass to tidal flat (**a**, **d**, **g**); Sungei Buloh—mangrove to tidal flat (**b**, **e**, **h**); and Sungei Puaka—mangrove to tidal flat (**c**, **f**, **i**). All transects start in vegetated components (negative plot values) and end in unvegetated portions (positive plot values). All solid lines indicate fitted regressions (*see* Table 1 for details). Dashed vertical lines indicate inflection point in sigmoidal regressions (**a**–**f**) or the maximum in peak models (**h**, **i**). All blue or green boxes indicate the area of transition for all sigmoidal and peak regression models. Dotted lines with shaded intervals indicate 95% confidence interval.

Table 1. Summary of statistical models' parameters used to describe aboveground cover, soil total organic carbon, and carbon dioxide fluxes across all locations by plot unless otherwise noted. AoT is the area of transition—*see* Data analysis section for details.

	Model type	R^2	Inflection point (m)	AoT (min)	AoT (max)
Seagrass cover (%)—Chek Jawa	Sigmoidal	0.833	−0.042	−0.204	0.120
Mangrove cover (%)—Sungei Buloh	Sigmoidal	0.933	0.849	−0.584	2.281
Mangrove cover (%)—Sungei Puaka	Sigmoidal	0.953	0.666	−0.323	1.654
Seagrass TOC (kg m^{-2})—Chek Jawa	NS				
Mangrove TOC (kg m^{-2})—Sungei Buloh	Sigmoidal	0.259	1.631	0.186	3.076
Mangrove TOC (kg m^{-2})—Sungei Puaka	Sigmoidal	0.160	2.052	−2.424	6.528
	Model type	R^2	p	**Peak location (m)**	**Peak width (m)**
Seagrass CO_2 flux (μmol m^{-2} s^{-1})—Chek Jawa	Linear	0.265	<0.001	NA	NA
Mangrove CO_2 flux (μmol m^{-2} s^{-1})—Sungei Buloh	Lorentzian peak	0.352	NA	−8.162	8.346
Mangrove CO_2 flux (μmol m^{-2} s^{-1})—Sungei Puaka	Lorentzian peak	0.232	NA	−4.370	4.303
Mangrove pneumatophore × CO_2 flux (μmol m^{-2} s^{-1})—Sungei Buloh	Exponential	0.473	<0.001	NA	NA
Mangrove pneumatophore × CO_2 flux (μmol m^{-2} s^{-1})—Sungei Puaka	Exponential	0.307	<0.001	NA	NA

Soil carbon storage

Total organic carbon of the measured soil profile showed a declining sigmoidal pattern across both mangrove to tidal flat transitions when integrated over depth, but seagrass to tidal flat transitions did not show a robust pattern and had a large amount of variability. The seagrass bed had values from ~ 10–20 kgTOC m^{-2} across the entire transition (Fig. 3d). Along both mangrove to tidal flat transitions the mangrove areas maintained on average 40–45 kgTOC m^{-2} and the adjacent tidal flats maintained on average 30–35 kgTOC m^{-2} (Fig. 3e,f). Both mangrove transitions had inflection points in similar locations along the transect at ~ 1.6–2.1 m into the tidal flat (Fig. 3e,f; Table 1). Sungei Buloh's area of transition for soil carbon was relatively discrete with a width of ~ 3.3 m, while Sungei Puaka's area of transition was much more gradual with a width of nearly 9 m in our model (Fig. 3e,f; Table 1). Sungei Buloh, however, had a larger range of variability in measured TOC values, especially in mangrove areas within 4 m of the tidal flat transition and both locations showed the greatest variability in areas surrounding either side of the aboveground transition.

Atmospheric CO_2 flux at soil surface

Carbon dioxide flux in seagrass to tidal flat transitions followed an increasing linear trend with interior seagrass bed endpoints (−8 m or less) having the most negative values at ~ −1 μmol m^{-2} s^{-1} and the tidal flat endpoints (8 m or more) approaching a neutral carbon dioxide flux (0 μmol m^{-2} s^{-1}) (Fig. 3g; Table 1). Mangrove to tidal flat transitions, however, followed a Lorentzian peak distribution for carbon dioxide soil flux and generally remained positive for both Sungei Buloh (Fig. 3h) and Sungei Puaka (Fig. 3i; Table 1) with only a few values slightly below zero. Both mangrove sites saw their peak flux values (> 3 μmol m^{-2} s^{-1}) within the mangrove forest at −8.2 m and − 4.4 m from the aboveground transition for the Sungei Buloh and Sungei Puaka location, respectively. Sungei Buloh's carbon dioxide flux peak width was also wider compared to the Sungei Puaka which had a far more discrete peak (Table 1). At both locations flux values across the transition in the tidal flats saw declines to rates of ~ 0.5–1 μmol m^{-2} s^{-1} and interior mangrove forest locations saw declines to rates of 1–2 μmol m^{-2} s^{-1} of CO_2 (Fig. 3h,i). It is important to note that flux values varied greatly across the ecotones and that at the transition the model fit was not as strong (overall R^2 0.23–0.35; Table 1). Carbon dioxide fluxes were further compared to pneumatophore density in mangrove to tidal flat transitions and both saw an exponential relationship with increasing pneumatophore density resulting in greater carbon dioxide fluxes (Fig. 4a,b).

Mapping of carbon stocks across the local seascape

We compared simple carbon stock evaluation techniques (i.e., simple estimate type) that only use estimates from interior portions of the respective ecosystems (Fig. 5a,b) to our estimates of carbon stock values (Fig. 5c,d) (i.e., ecotone estimate type) which were interpolated and extrapolated using regression values across the ecotone and mapped at a spatial landscape scale for each of our three locations. This was only done for the two mangrove transitions as the seagrass transition did not see significant differences in the regression

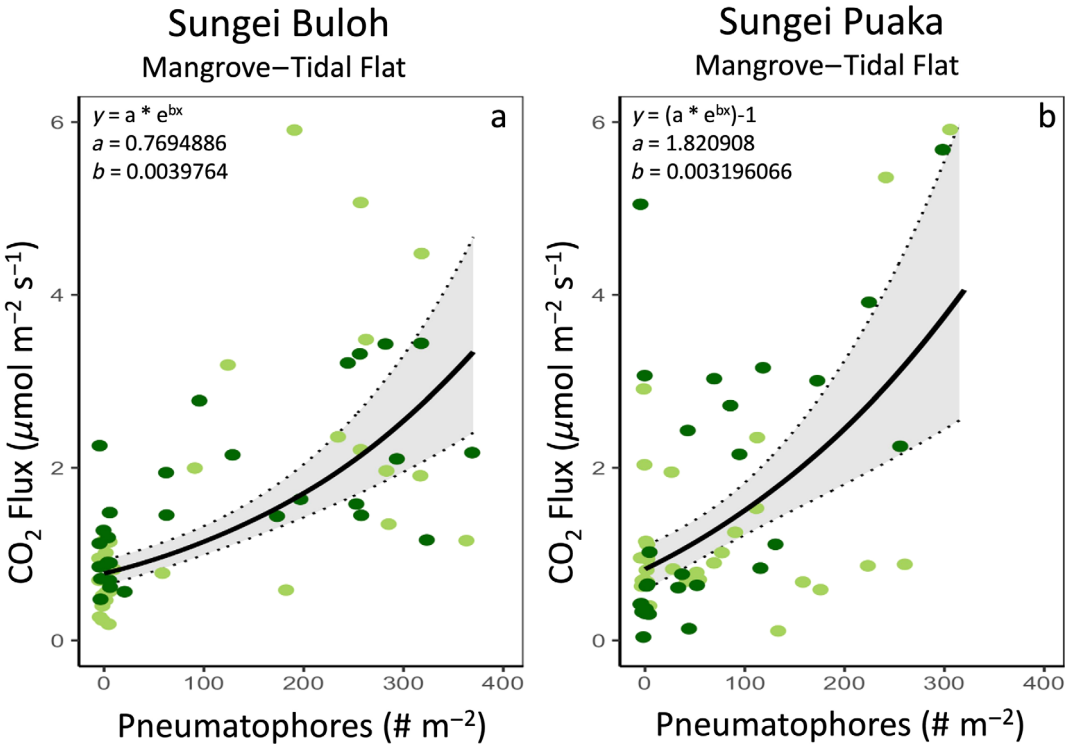

Fig. 4. Carbon dioxide flux (μmol m^{-2} s^{-1}) compared to pneumatophore density (# m^{-2}) for Sungei Buloh (**a**) and Sunge Puaka (**b**). Regression information found in Table 1. Light green dots are from 2020 measurements and dark green dots are from 2021 measurements. Equations and coefficients in top left portion and dotted lines with shaded interval indicate 95% confidence interval.

analysis. The difference in estimated values of carbon stock per area (kg m^{-2}) were largest at the habitat edges, especially at the Sungei Puaka mangrove–tidal flat site (Fig. 5c,f). Differences at the Sungei Buloh mangrove–tidal flat site were less substantial, but still present (Fig. 5b,e). When comparing the overall totals of estimates at the patch level we found that changes were small (± 1%), but within habitat differences were more pronounced. In Sungei Puaka, mangrove carbon stocks were overestimated by 2% and tidal flat carbon stocks were underestimated by 4%, while in Sungei Buloh mangrove carbon stocks were overestimated by 0.2% and tidal flat carbon stocks were underestimated by 8%.

Discussion

We examined ecotones between vegetated and unvegetated portions of the coastal seascape and analyzed the differences between aboveground boundaries and belowground carbon storage and fluxes. Aboveground boundaries in seagrass and mangrove ecosystems were relatively concise and rapidly transitioned in their vegetation cover from vegetated portions to adjacent unvegetated areas following a sigmoidal pattern. Belowground carbon storage and flux values, however, ranged in the shape and rate of their transition between the vegetated and unvegetated areas and differed depending on the ecosystems being examined. Translated to the local seascape, these patterns highlight the importance of understanding transitional zones to better understand edge impacts and heterogeneity/variability and contribute to a more accurate estimate of these critical ecosystem properties (carbon storage) and processes (carbon dioxide flux).

Soil carbon storage vs. aboveground vegetation

In the seagrass-tidal flat transitions, we found no significant change in carbon stocks in adjacent tidal flat locations and at the edges of the seagrass bed compared to interior seagrass bed locations, but we did find greater variability. This is quite different from the aboveground portions and warrants further exploration of the sources of carbon as tidal flats commonly maintain lower amounts of carbon compared to seagrasses (Ricart et al. 2015). Potential sources of carbon at edge and tidal flat portions could be landward mangroves, previous seagrass beds, benthic algae contributions, or allochthonous carbon sources via river or tidal deposition from terrestrial or marine sources (Kennedy et al. 2010; Oreska et al. 2018). Many of the seagrass species present at the site are pioneer species (Yaakub et al. 2013) which may limit the amount of carbon stored in the soil and their ability to sequester and store carbon due to their small stature, recent establishment, and sometimes ephemeral nature (Alemu et al. 2022). Sediment grain size is another known potential control to carbon storage (Kelleway et al. 2016) in coastal sediments with this

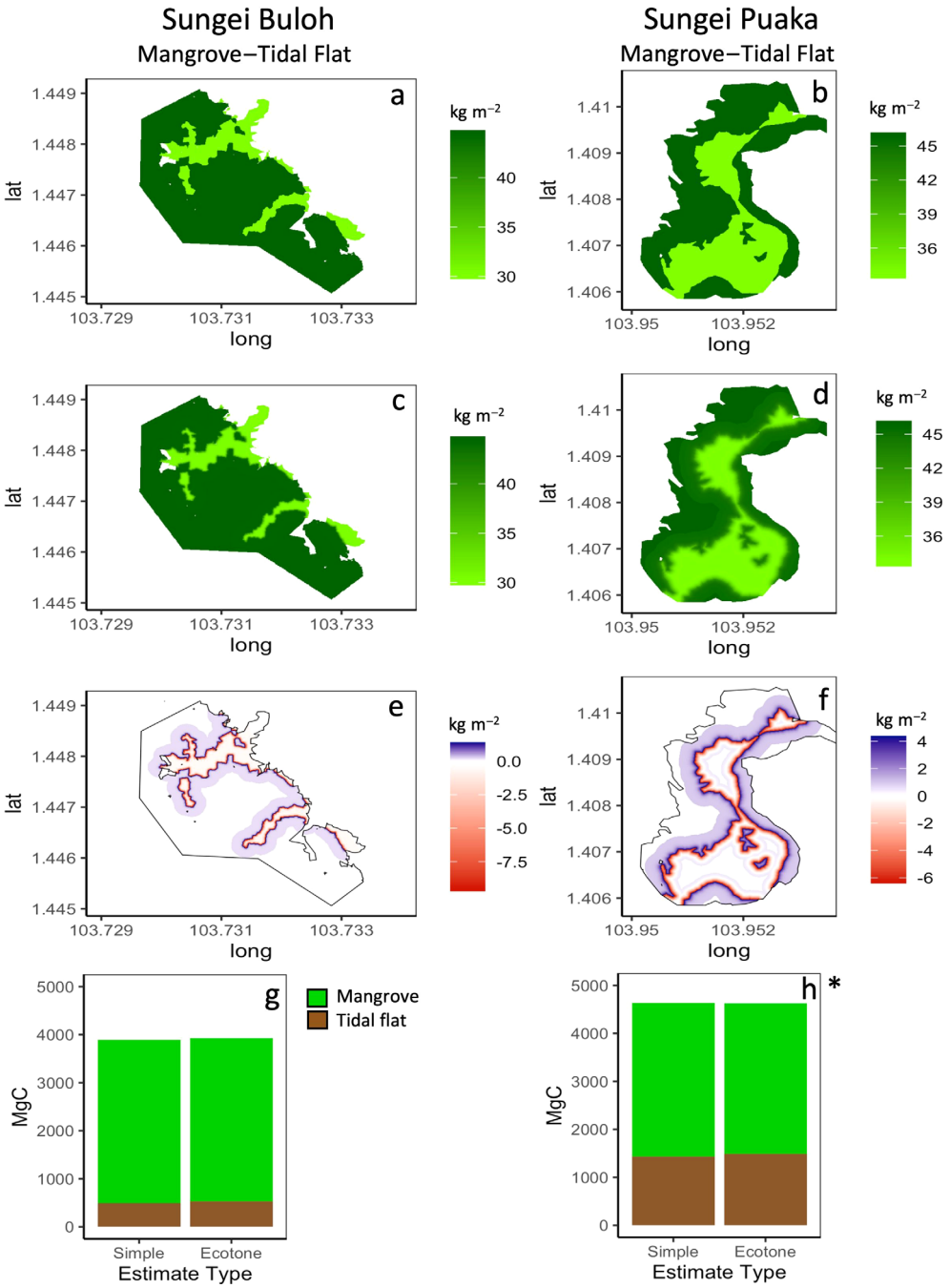

Fig. 5. Mapped soil carbon stocks (kgC m^{-2}) using simple estimates (**a**, **b**), ecotone-specific estimates (**c**, **d**), the over or under estimation of simple carbon estimates to ecotone estimates (**e**, **f**), and a comparison of the two estimate types by habitat type (**g**, **h**) for Sungei Buloh (mangrove–tidal flat) (left) and Sungei Puaka (mangrove–tidal flat) (right). For over or under estimations of simple carbon estimates to ecotone estimates, over estimations are in blue (positive values) and underestimations are in red (negative values) with zero values shown in white (**e**, **f**). For total estimate comparison mangrove in green, and tidal flat in brown. * indicates the same legend that is present in panel (**g**) can be applied to panel (**h**).

area maintaining patches of both sand and finer silts/muds. Several previous studies on the site also examined various blue carbon storage components of both seagrass beds (Alemu et al. 2022) and across the broader seascape (Phang et al. 2015; Saavedra-Hortua et al. 2020) and similarly found that seagrasses contain low levels of carbon and the unvegetated tidal flats often contain similar or slightly higher values. Overall, our values are lower than global means (Fourqurean et al. 2012). Seascape arrangement has also been observed to play a significant role in carbon storage in seagrass

systems elsewhere with seagrass beds adjacent to mangroves receiving allochthonous subsidies (Asplund et al. 2021). Previous work in other areas has found the opposite trend as our study with adjacent areas and seagrass edges having less carbon than interior portions (Ricart et al. 2015), but these systems may have been more established or not have had nearby mangrove forest patches/other subsidies. Our values may reflect more recent changes in either ecosystem distribution, sediment dynamics, disturbances, or other changes that impact carbon accumulation.

In mangroves, soil carbon storage has been shown to be greater in interior portions of mangrove patches compared to fringes (Simpson et al. 2017; Sasmito et al. 2020) with our findings showing a similar overall trend and providing additional spatial resolution to the decrease across the aboveground ecotone into the surrounding tidal flats. Whereas aboveground vegetation cover transitions were relatively concise with narrow transition zones, belowground carbon stock transitions maintained a wider sigmoidal transition with broader but differing areas of transition, perhaps due to differences in site geomorphology and wave energy. For both sites we found that adjacent portions of tidal flats (0–4 m from aboveground transition) contained similar levels of stored soil carbon compared to the edge portions of mangroves. These findings add finer scale resolution to both experimental and conceptual work examining overflow of carbon from blue carbon ecosystems into nearby areas (Huxham et al. 2018; Bulmer et al. 2020; Yan et al. 2024). In addition to cross boundary subsidies from other terrestrial or marine systems, this may also be due to previous blue carbon ecosystem extent (Kelleway et al. 2017), historical terrestrial peat systems (Stevenson et al. 2022), belowground root subsidies into surrounding sediments (Yando et al. 2018), or faunal redistribution of sediments through burrowing or digging (Xiao et al. 2020; Agusto et al. 2022). While soil carbon stocks showed a wider area of transition than aboveground portions, the transition occurred over a smaller distance compared to other studies that examined fringing mangroves at a coarser resolution (Sasmito et al. 2020). The relatively discrete edges observed in this study may be due to the broader geomorphic setting and anthropogenic impacts that resulted in relatively narrow mangrove patches compared to other highly extensive mangrove forests found elsewhere in Southeast Asia. Mangrove–tidal flat ecotonal areas, −5 to 5 m on the transects, also saw larger amounts of variability at the aboveground transition compared to interior portions (*see* Fig. 3e,f). This may be due to the capture of subsidies from both seaward and landward portions of the seascape (logs, sand or wrack deposits, trapped litter, etc., personal observation), previously existing mangrove extent that has been reduced due to erosion/degradation (Kelleway et al. 2017), or the dynamic nature of edges. Our work further emphasizes heterogeneity within the systems particularly at the edges and the importance of robust sampling efforts so as not to over- or underestimate stocks. While carbon stock values at these sites were greater than previous work done in Singapore for both mangroves and tidal flats (Phang et al. 2015) these stock estimates are still on the overall lower end of soil carbon stocks for mangroves globally (Kauffman et al. 2020; MacKenzie et al. 2021), which may reflect the disturbance history (direct and indirect) of urban mangroves, including historical harvesting, pollution, shrimp ponds, land reclamation efforts, industry, and nearby dredging (Hilton and Manning 1995; Friess et al. 2012).

Atmospheric CO_2 flux at soil surface

Our carbon dioxide flux results showcase a small, but statistically significant increase from within the seagrass beds, across the aboveground ecotone and into the surrounding tidal flat. This response is largely expected, as sequestration was occurring due to photosynthesis during low tide measurements in the seagrass bed. Carbon dioxide flux within mangrove–tidal flat transitions maintained a Lorentzian peak distribution at both locations with a maximum flux just within the mangrove forest in both years sampled. We are confident that our measurements are accurate with this unexpected pattern but acknowledge that our sampling was also restricted to low tide. Pneumatophores likely play a role in this flux peak as pneumatophore density was correlated to carbon dioxide flux following an exponential increase (Fig. 4a,b). While pneumatophores are well known for their ability to allow for gas exchange (Scholander et al. 1955; Björn et al. 2022), a spatial examination of their gas exchange has not previously been explored to our knowledge. Pneumatophores in this study were from the *Avicennia* genus (*A. alba* and *A. officinalis*), a genus commonly found in tidal flat adjacent portions of the mangrove forest (described in Singapore by Leong et al. 2018). The flux values we measured were similar to those seen by Simpson et al. (2019) who measured at the interior and fringe of mangrove patches in Florida; we further observed similar increases in variability at and around the aboveground transition as their work. Values from other studies commonly show elevated fluxes in] mangrove habitats compared to adjacent unvegetated areas (Martin et al. 2020), although this was minor when comparing interior portions of the mangrove and interior tidal flat locations. To gain a fully comprehensive understanding of fluxes in all of these systems we would need to sample throughout the tidal cycle as well as the respective adjacent portions of the seascape (Call et al. 2015). Understanding flux measurements in blue carbon systems is a common challenge, but highly needed for accounting and refining carbon budgets in these systems and the broader seascape (Bouillon et al. 2008; Macreadie et al. 2021) and specifically in southeast Asia (Sharma et al. 2023).

Implications of spatial variation when extrapolating to the seascape

Aboveground extent via habitat maps is most commonly used to extrapolate average values from interior portions of patches in blue carbon assessments, with minimal

incorporation of heterogeneity from interior to edge across those habitats. Patch edges have been shown to have differences from the patch interior regarding structure, function, and communities in both mangrove and seagrass (Lovelock et al. 2005; Yarnall et al. 2022). Our findings suggest that heterogeneity across habitat ecotones should be considered in blue carbon assessments when possible as our study saw differences of 0%–8% from traditional assessments. Our use of high-frequency sampling, paired with regression and subsequent extrapolation, provides increased resolution in portions of the seascape that are likely to have the greatest heterogeneity as seen in our measurements. The differences in estimates in our mangrove–tidal flat transitions showcase the overestimation of mangrove soil carbon (− 0.2%–2%; 8–70 MgC) and underestimation of tidal flat carbon in mangrove adjacent areas (3%–8%; 38–58 MgC). Our model estimates are not without their own uncertainties as the data used to produce these models maintained variability. The overall ability to provide increased accuracy for carbon estimates, however, is particularly salient in highly fragmented habitats and in the context of the broader seascape (Call et al. 2015; Krause et al. 2022). Further this work highlights the need to account for not only ecotonal areas, but also consider the importance of nonvegetated habitats, especially in proximal locations to vegetated portions (Lovelock and Reef 2020; Sasmito et al. 2020). These nonvegetated systems may store carbon derived from blue carbon ecosystems whether it is through transport or habitat migration, with the latter being particularly important with sea level rise. In addition to systems adjacent to blue-carbon habitats presently, unvegetated tidal flats may also be found in developed areas where blue carbon habitats previously existed and may continue to store some of the carbon sequestered by those former ecosystems, yielding another reason to protect and maintain unvegetated portions of the seascape (Meijer et al. 2021; Krause et al. 2022; Al Disi et al. 2023).

Conclusions

This research builds upon previous work examining multiple coastal ecosystems in the context of their position in the seascape with a focus on heterogeneity, something that has been a staple of habitat usage studies (Bostrom et al. 2011), but has only recently been examined for carbon storage and sequestration. This work paired with others examining seascape impacts (e.g., Huxham et al. 2018; Bulmer et al. 2020; Krause et al. 2022) provides important context at the micro- and meso-spatial scale. Understanding the importance of patch sizes, aggradation, and arrangement remains to be understood in blue carbon ecosystems. Further, understanding the scale at which ecotone dynamics are important is critical, as large spatial scales and systems with small perimeter-area ratios will likely see small differences in net system carbon stock and sequestration estimates. Finally, we must acknowledge that this method of sampling is both labor and financially intensive. The need for incorporating heterogeneity and accounting for ecotonal and edge effects into blue carbon and ecosystem service assessments is paramount to bridging the gap between plot-based studies and seascape scale estimates. With additional studies there is a possibility that correction factors to account for ecotone impacts could be developed, but this requires greater investigation in other systems to determine if similar patterns are observed in other geographic and geomorphic regions as well as salt marshes. By refining our understanding of carbon stocks and sequestration we can further understand both the pattern and process of these critical ecosystems and their influence on the coastal seascape.

Data availability statement

All data and example code is available on GitHub (Yando et al. 2024; DOI: 10.5281/zenodo.13863628).

References

Agusto, L. E., and others. 2022. Fiddling with the blue carbon: Fiddler crab burrows enhance CO_2 and CH4 efflux in saltmarsh. Ecol. Indic. **1**: 109538.

Al Disi, Z. A., and others. 2023. Variability of blue carbon storage in arid evaporitic environment of two coastal sabkhas or mudflats. Sci. Rep. **13**: 12723.

Alemu, J. B., S. M. Yaakub, E. S. Yando, R. Y. San Lau, C. C. Lim, J. Y. Puah, and D. A. Friess. 2022. Geomorphic gradients in shallow seagrass carbon stocks. Estuar. Coast. Shelf Sci. **265**: 107681.

Arriola, J. M., and J. E. Cable. 2017. Variations in carbon burial and sediment accretion along a tidal creek in a Florida salt marsh. Limnol. Oceanogr. **62**: S15–S28.

Asplund, M. E., and others. 2021. Dynamics and fate of blue carbon in a mangrove–seagrass seascape: Influence of landscape configuration and land-use change. Landsc. Ecol. **36**: 1489–1509.

Barbier, E., S. Hacker, C. Kennedy, E. Koch, A. Stier, and B. Silliman. 2011. The value of estuarine and coastal ecosystem services. Ecol. Monogr. **81**: 169–193. doi:10.1890/10-1510.1

Behera, M. R., C. Chun, S. Palani, and P. Tkalich. 2013. Temporal variability and climatology of hydrodynamic, water property and water quality parameters in the West Johor Strait of Singapore. Mar. Pollut. Bull. **77**: 380–395.

Björn, L. O., B. A. Middleton, M. Germ, and A. Gaberščik. 2022. Ventilation systems in wetland plant species. Diversity **14**: 517.

Bostrom, C., S. J. Pittman, C. Simenstad, and R. T. Kneib. 2011. Seascape ecology of coastal biogenic habitats: Advances, gaps, and challenges. Mar. Ecol. Prog. Ser. **427**: 191–217. doi:10.3354/meps09051

Bouillon, S., and others. 2008. Mangrove production and carbon sinks: A revision of global budget estimates. Global Biogeochem. Cycles **22**:GB013

Bulmer, R. H., F. Stephenson, H. F. E. Jones, M. Townsend, J. R. Hillman, L. Schwendenmann, and C. Lundquist. 2020. Blue carbon stocks and cross-habitat subsidies. Front. Mar. Sci. **7**: 380.

Call, M., and others. 2015. Spatial and temporal variability of carbon dioxide and methane fluxes over semi-diurnal and spring–neap–spring timescales in a mangrove creek. Geochim. Cosmochim. Acta **150**: 211–225.

Cheng, J., B. Karambelkar, and Y. Xie. 2022. leaflet: Create interactive web maps with the JavaScript. Available from https://rstudio.github.io/leaflet/

Engelbrecht, T., S. von der Heyden, and A. Ndhlovu. 2024. Blue carbon dynamics across a salt marsh-seagrass ecotone in a cool-temperate estuary. Plant Soil. doi:10.1007/s11104-024-06953-8

Fourqurean, J. W., and others. 2012. Seagrass ecosystems as a globally significant carbon stock. Nat. Geosci. **5**: 505–509.

Friess, D. A. 2017. Mangrove rehabilitation along urban coastlines: A Singapore case study. Reg. Stud. Mar. Sci. **16**: 279–289.

Friess, D. A., J. Phelps, R. C. Leong, W. K. Lee, A. K. S. Wee, N. Sivasoth, R. R. Y. Oh, and E. L. Webb. 2012. Mandai mangrove, Singapore: Lessons for the conservation of Southeast Asia's mangroves. Raffles Bull. Zool. **25**: 55–65.

Gosz, J. R. 1993. Ecotone hierarchies. Ecol. Appl. **3**: 370–376. doi:10.2307/1941905

Hijmans, R. 2023. Terra: Spatial data analysis. R package (v. 1.7-27). Available from https://rspatial.org/

Hilton, M. J., and S. S. Manning. 1995. Conversion of coastal habitats in Singapore: Indications of unsustainable development. Environ. Conserv. **22**: 307–322.

Holland, M., P. G. Risser, and R. J. Naiman [eds.]. 1991. Ecotones: The role of landscape boundaries in the management and restoration of changing environments. Chapman and Hall.

Howard, J., Hoyt, S., Isensee, K., Telszewski, M. and Pidgeon, E., 2014. Coastal blue carbon: methods for assessing carbon stocks and emissions factors in mangroves, tidal salt marshes, and seagrasses, 180 p. Conservation International, Intergovernmental Oceanographic Commission ofUNESCO, International Union for Conservation of Nature.

Hufkens, K., R. Ceulemans, and P. Scheunders. 2008. Estimating the ecotone width in patchy ecotones using a sigmoid wave approach. Eco. Inform. **3**: 97–104. doi:10.1016/j.ecoinf.2008.01.001

Huxham, M., D. Whitlock, M. Githaiga, and A. Dencer-Brown. 2018. Carbon in the coastal seascape: How interactions between mangrove forests, seagrass meadows and tidal marshes influence carbon storage. Curr. For. Rep. **4**: 101–110. doi:10.1007/s40725-018-0077-4

Hyndes, G. A., I. Nagelkerken, R. J. McLeod, R. M. Connolly, P. S. Lavery, and M. A. Vanderklift. 2014. Mechanisms and ecological role of carbon transfer within coastal seascapes. Biol. Rev. **89**: 232–254. doi:10.1111/brv.12055

Kauffman, J. B., C. Heider, T. G. Cole, K. A. Dwire, and D. C. Donato. 2011. Ecosystem carbon stocks of Micronesian mangrove forests. Wetlands **31**: 343–352.

Kauffman, J. B., and D. C. Donato. 2012. Protocols for the measurement, monitoring and reporting of structure, biomass and carbon stocks in mangrove forests, v. **86**. CIFOR.

Kauffman, J. B., M. F. Adame, V. B. Arifanti, L. M. Schile-Beers, A. F. Bernardino, R. K. Bhomia, and D. C. Donato. 2020. Total ecosystem carbon stocks of mangroves across broad global environmental and physical gradients. Ecol. Monogr. **90**: e01405.

Kelleway, J. J., N. Saintilan, P. I. Macreadie, and P. J. Ralph. 2016. Sedimentary factors are key predictors of carbon storage in SE Australian saltmarshes. Ecosystems **19**: 865–880.

Kelleway, J. J., N. Saintilan, P. I. Macreadie, J. A. Baldock, and P. J. Ralph. 2017. Sediment and carbon deposition vary among vegetation assemblages in a coastal salt marsh. Biogeosciences **14**: 3763–3779.

Kennedy, H., J. Beggins, C. M. Duarte, J. W. Fourqurean, M. Holmer, N. Marbà, and J. J. Middelburg. 2010. Seagrass sediments as a global carbon sink: Isotopic constraints. Global Biogeochem. Cycles **24**: GB4026

Krause, J. R., A. Hinojosa-Corona, A. B. Gray, J. C. Herguera, J. McDonnell, M. V. Schaefer, S. C. Ying, and E. B. Watson. 2022. Beyond habitat boundaries: Organic matter cycling requires a system-wide approach for accurate blue carbon accounting. Limnol. Oceanogr. **67**: S6–S18. doi:10.1002/lno.12071

Lai, S., L. H. L. Loke, M. J. Hilton, T. J. Bouma, and P. A. Todd. 2015. The effects of urbanisation on coastal habitats and the potential for ecological engineering: A Singapore case study. Ocean Coast. Manag. **103**: 78–85. doi:10.1016/j.ocecoaman.2014.11.006

Leong, R. C., D. A. Friess, B. Crase, W. K. Lee, and E. L. Webb. 2018. High-resolution pattern of mangrove species distribution is controlled by surface elevation. Estuar. Coast. Shelf Sci. **202**: 185–192.

Lovelock, C. E., I. C. Feller, K. L. McKee, and R. C. Thompson. 2005. Variation in mangrove forest structure and sediment characteristics in Bocas del Toro, Panama. Caribb. J. Sci. **41**: 456–464.

Lovelock, C. E., and C. M. Duarte. 2019. Dimensions of blue carbon and emerging perspectives. Biol. Lett. **15**: 20180781. doi:10.1098/rsbl.2018.0781

Lovelock, C. E., and R. Reef. 2020. Variable impacts of climate change on blue carbon. One Earth **3**: 195–211.

MacKenzie, R., S. Sharma, and A. R. Rovai. 2021. Environmental drivers of blue carbon burial and soil carbon stocks in

mangrove forests, p. 275–294. *In* Dynamic sedimentary environments of mangrove coasts. Elsevier.

Macreadie, P. I., and others. 2019. The future of blue carbon science. Nat. Commun. **10**: 1–13. doi:10.1038/s41467-019-116.93-w

Macreadie, P.I., Costa, M.D., Atwood, T.B., Friess, D.A., Kelleway, J.J., Kennedy, H., Lovelock, C.E., Serrano, O. and C.M. Duarte. 2021. Blue carbon as a natural climate solution. Nat. Reviews Earth & Environ. **2**(12): 826–839

Martin, R. M., C. Wigand, A. Oczkowski, A. Hanson, S. Balogh, B. Branoff, E. Santos, and E. Huertas. 2020. Greenhouse gas fluxes of mangrove soils and adjacent coastal waters in an urban, subtropical estuary. Wetlands **40**: 1469–1480. doi:10.1007/s13157-020-01300-w

Masante, D. 2016. landscapeR: Categorical landscape simulation facility. R package version 1.1.2. Available from https://cran.r-project.org/package=landscapeR

McLeod, E., and others. 2011. A blueprint for blue carbon: Toward an improved understanding of the role of vegetated coastal habitats in sequestering CO_2. Front. Ecol. Environ. **9**: 552–560. doi:10.1890/110004

Meijer, K. J., E. H. M. El-Hacen, L. L. Govers, M. Lavaleye, T. Piersma, and H. Olff. 2021. Mangrove-mudflat connectivity shapes benthic communities in a tropical intertidal system. Ecol. Indic. **130**: 108030.

Meteorological Service of Singapore. 2024. Climate of Singapore. [accessed 2024 August 1]. Available from https://www.weather.gov.sg/climate-climate-of-singapore/

Nakagawa, S., P. C. Johnson, and H. Schielzeth. 2017. The coefficient of determination R^2 and intra-class correlation coefficient from generalized linear mixed-effects models revisited and expanded. J. R. Soc. Interface **14**: 20170213.

Odum, E. P. 1968. A research challenge: Evaluating the productivity of coastal and estuarine water, p. 63–64. *In* Proceedings of the second sea grant conference. Univ. of Rhode Island.

Oreska, M. P., G. M. Wilkinson, K. J. McGlathery, M. Bost, and B. A. McKee. 2018. Non-seagrass carbon contributions to seagrass sediment blue carbon. Limnol. Oceanogr. **63**: S3–S18.

Owers, C. J., C. D. Woodroffe, D. Mazumder, and K. Rogers. 2022. Carbon storage in coastal wetlands is related to elevation and how it changes over time. Estuar. Coast. Shelf Sci. **267**: 107775.

Phang, V. X., L. M. Chou, and D. A. Friess. 2015. Ecosystem carbon stocks across a tropical intertidal habitat mosaic of mangrove forest, seagrass meadow, mudflat and sandbar. Earth Surf. Process. Landf. **40**: 1387–1400.

Ricart, A. M., P. H. York, M. A. Rasheed, M. Pérez, J. Romero, C. V. Bryant, and P. Macreadie. 2015. Variability of sedimentary organic carbon in patchy seagrass landscapes. Mar. Pollut. Bull. **100**: 476–482.

Ricart, A. M., M. Pérez, and J. Romero. 2017. Landscape configuration modulates carbon storage in seagrass sediments. Estuar. Coast. Shelf Sci. **185**: 69–76.

Ricart, A. M., P. H. York, C. V. Bryant, M. A. Rasheed, D. Ierodiaconou, and P. Macreadie. 2020. High variability of blue carbon storage in seagrass meadows at the estuary scale. Sci. Rep. **10**: 5865.

Rovai, A. S., and others. 2018. Global controls on carbon storage in mangrove soils. Nat. Clim. Change **8**: 534–538.

RStudio Team (2024). RStudio: Integrated Development for R. RStudio, PBC, Boston, MA URL http://www.rstudio.com/.

Saavedra-Hortua, D. A., D. A. Friess, M. Zimmer, and L. G. Gillis. 2020. Sources of particulate organic matter across mangrove forests and adjacent ecosystems in different geomorphic settings. Wetlands **40**: 1047–1059.

Sasmito, S. D., Y. Kuzyakov, A. A. Lubis, D. Murdiyarso, L. B. Hutley, S. Bachri, D. A. Friess, C. Martius, and N. Borchard. 2020. Organic carbon burial and sources in soils of coastal mudflat and mangrove ecosystems. Catena **187**: 104414. doi:10.1016/j.catena.2019.104414

Scholander, P. F., L. Van Dam, and S. I. Scholander. 1955. Gas exchange in the roots of mangroves. Am. J. Bot. **42**: 92–98.

Sharma, S., R. Ray, C. Martius, and D. Murdiyarso. 2023. Carbon stocks and fluxes in Asia-Pacific mangroves: Current knowledge and gaps. Environ. Res. Lett. **18**: 044002.

Simpson, L. T., T. Z. Osborne, L. J. Duckett, and I. C. Feller. 2017. Carbon storage along a climate induced coastal wetland gradient. Wetlands **37**: 1023–1035.

Simpson, L. T., T. Z. Osborne, and I. C. Feller. 2019. Wetland soil CO_2 efflux along a latitudinal gradient of spatial and temporal complexity. Estuaries Coast **42**: 45–54. doi:10.1007/s12237-018-0442-3

Stevenson, A., T. C. Ó Corcora, W. Hukriede, P. R. Schubert, and T. B. Reusch. 2022. Substantial seagrass blue carbon pools in the southwestern Baltic Sea include relics of terrestrial peatlands. Front. Mar. Sci. **9**: 949101.

Strayer, D. L., M. E. Power, W. F. Fagan, S. T. A. Pickett, and J. Belnap. 2003. A classification of ecological boundaries. Bioscience **53**: 723. doi:10.1641/0006-3568(2003)053[0723:ACOEB]2.0.CO;2

Systat. 2023. SigmaPlot v. 12.5. Systat Software Inc.

Taillardat, P., D. A. Friess, and M. Lupascu. 2018. Mangrove blue carbon strategies for climate change mitigation are most effective at the national scale. Biol. Lett. **14**: 20180251. doi:10.1098/rsbl.2018.0251

Tan, Y. J., and others. 2023. Remote sensing mapping of the regeneration of coastal natural habitats in Singapore: Implications for marine conservation in tropical cities. Singap. J. Trop. Geogr. **44**: 130–148.

Timoney, K., G. La Roi, and M. R. Dale. 1993. Subarctic forest-tundra vegetation gradients: The sigmoid wave hypothesis. J. Veg. Sci. **4**: 387–394. doi:10.2307/3235597

Titlyanova, A. A., I. P. Romanova, N. P. Kosykh, and N. P. Mironycheva-Tokareva. 1999. Pattern and process in above-ground and below-ground components of grassland ecosystems. J. Veg. Sci. **10**: 307–320. doi:10.2307/3237060

Wiens, J. A., C. S. Crawford, and J. R. Gosz. 1985. Boundary dynamics: A conceptual framework for studying landscape ecosystems. Oikos **45**: 421–427. doi:10.2307/3565577

Woodroffe, C. D., K. Rogers, K. L. McKee, C. E. Lovelock, I. A. Mendelssohn, and N. Saintilan. 2016. Mangrove sedimentation and response to relative sea-level rise. Ann. Rev. Mar. Sci. **8**: 243–266. doi:10.1146/annurev-marine-122414-034025

Wyrtki, K. 1961. Physical oceanography of the southeast Asian waters, v. **2**. Univ. of California, Scripps Institution of Oceanography.

Xiao, K., and others. 2020. Large CO_2 release and tidal flushing in salt marsh crab burrows reduce the potential for blue carbon sequestration. Limnol. Oceanogr. **66**: 14–29.

Yaakub, S. M., R. L. Lim, W. L. Lim, and P. A. Todd. 2013. The diversity and distribution of seagrass in Singapore. Nat. Singap. **6**: 105–111.

Yaakub, S. M., L. J. McKenzie, P. L. A. Erftemeijer, T. Bouma, and P. A. Todd. 2014. Courage under fire: Seagrass persistence adjacent to a highly urbanised city-state. Mar. Pollut. Bull. **83**: 417–424. doi:10.1016/j.marpolbul.2014.01.012

Yan, R., and others. 2024. Spatial variation of organic carbon storage and aggregate sizes in the sediment of the Zhangjiang mangrove ecosystem. Catena **234**: 107545.

Yando, E. S., I. J. B. Alemu, K. E. Lim, T. M. Sloey, M. van Breugel, N. Bhatia, and D. A. Friess. 2024. Data for "Edge effects impact blue carbon dynamics across coastal ecotones in a tropical seascape." Zenodo. Available from https://doi.org/10.5281/zenodo.13863629

Yando, E. S., M. J. Osland, and M. W. Hester. 2018. Microspatial ecotone dynamics at a shifting range limit: Plant–soil variation across salt marsh–mangrove interfaces. Oecologia **187**: 319–331. doi:10.1007/s00442-018-4098-2

Yang, S., R. L. F. Lim, C. F. Sheue, and J. W. H. Yong. 2011. The current status of mangrove forests in Singapore, p. 99–120. *In* Proceedings of nature society, Singapore's conference on "Nature conservation for a sustainable Singapore". Nature Society Singapore.

Yarnall, A. H., J. E. Byers, L. A. Yeager, and F. J. Fodrie. 2022. Comparing edge and fragmentation effects within seagrass communities: A meta-analysis. Ecology **103**: e3603.

Young, M. A., O. Serrano, P. I. Macreadie, C. E. Lovelock, P. Carnell, and D. Ierodiaconou. 2021. National scale predictions of contemporary and future blue carbon storage. Sci. Total Environ. **800**: 149573. doi:10.1016/j.scitotenv.2021.149573

Acknowledgments

We extend our thanks to S. Chua, D. How, N. Nguyen, L. Wong, T. Hui, Y. Nathan, C. Tan, J. Saunders, V. Koh, A. Tan, T. Hui, J. Moore, M. Sillanpää, M.A. Bin Sani, and N. Choudhary for their assistance in the field and/or the lab, and the Pulau Ubin Community. Technical and analysis assistance was provided by E. Segovia, Y. Han, L.W. Wong (National University of Singapore), Y. Nathan (Nanyang Technological University), and W.R. James (Florida International University). We thank the National Parks Board and the Singapore Land Authority, Government of Singapore for site access (permit numbers: NP/RP19-016-1[a-d]). This research was supported by the National Research Foundation—Prime Minister's Office, Singapore under its Campus for Research Excellence and Technological Enterprise (CREATE) Programme via grant to DAF and NB, Singapore's Ministry of Education—International Collaborative Fellowship for the Commonwealth (NRF-CSC-ICFC2017-06) to JBA, and Singapore's Ministry of Education and Yale-NUS College (Grant IG19-SG113) via grant to MvB.

Conflict of Interest

None declared.

Submitted 14 March 2024
Revised 02 October 2024
Accepted 23 October 2024

Associate editor: Oscar Serrano